31st Annual International Conference of the IEEE EMBS
Minneapolis, Minnesota, USA, September 2-6, 2009

Assessment of Pulsatile Wall Shear Stress in Compliant Arteries: Numerical Model, Validation and Experimental Data

Fernando P. Salvucci, Carlos A. Perazzo, Juan G. Barra, and Ricardo L. Armentano

Abstract— **There is evidence that wall shear stress (*WSS*) is associated with vascular disease. In particular, it is widely accepted that vascular segments with low or oscillatory values of *WSS* are more probable to develop vascular disease. It is then necessary to establish a realistic model of the blood flow in blood vessels in order to determine precisely *WSS*.**

We proposed a numerical 1D model which takes into account the pulsatile nature of blood flow, the elasticity of the vessel, and its geometry. The model allows the calculation of shear stress. It was validated for stationary situations. Then, we computed the time–dependent *WSS* distribution from experimental data in the sheep thoracic aorta.

Results showed that mean *WSS* calculated through steady flow and rigid walls models is overestimated. Peak *WSS* values for pulsatile flow must be considered since they resulted to be at least one order higher than mean values. Oscillations in shear stress in a period showed to be approximately of 40%.

These findings show that the proposed model is suitable for estimating time–dependent *WSS* distributions, and confirm the need of using this kind of model when trying to evaluate realistic *WSS* in blood vessels.

I. INTRODUCTION

Wall shear stress (*WSS*) expresses the force per unit area exerted by a fluid in motion on a solid boundary in a direction on the local tangent plane. Currently, issues related to *WSS* distribution in arterial flow are receiving attention because of emerging evidence that it is associated with vascular disease [1][2][3]. Several studies have led to the notion that local hemodynamic factors, such as *WSS*, may play a role in the initiation and, perhaps, progression of the disease [1][2][3][4]. It is now widely accepted that the vessel segments that appear to be at the highest risk for development of diseases (such as atherosclerosis) are those with low or oscillatory *WSS* values [2][3]. It is then necessary to develop models that allow obtaining realistic *WSS* patterns in blood vessels [5].

Determination of *WSS* in the arterial flow is not trivial due to the complexity of the system under consideration. Firstly, the problem is described exactly by the three Navier–Stokes equations of motion for the fluid, the equation of continuity for the fluid, and equations of motion for the vessel wall. A general solution for such a system has not been achieved. Additionally, not all of the physiological quantities involved are easy to obtain in the practice.

Here we show how to achieve realistic time-dependent *WSS* values and distributions by means a 1D model for the blood flow which takes into account realistic features of the problem such as the vessel geometry (tapering), the flow nature (pulsatility) and the vessel wall properties (compliance). Additionally, we present results obtained with real data from an animal model.

F. P. Salvucci, C. A. Perazzo, J. G. Barra, and R. L. Armentano are with School of Engineering and Natural and Exact Sciences, Favaloro University, Buenos Aires, Argentina. fsalvucci@favaloro.edu.ar

II. MATERIALS AND METHODS

A. Model

We consider flow in a compliant tube with axial symmetry, which is the artery. This flow may be stated as quasi-one-dimensional. This means that the radial velocity v_r is much smaller than axial velocity v_z. In the case of flexible tubes (such as mammalian arteries) this is acceptable, since the maximum value of v_r is the radial velocity of the wall, which will be small unless the tube is very flexible [6]. We assume blood as a Newtonian fluid.

By neglecting the terms corresponding to v_r in the Navier–Stokes equations, averaging in the cross sectional area and considering the continuity equation for this case, one obtains the following system of equations [6]:

$$\frac{\partial U}{\partial t}+\frac{U}{A}(1-\alpha)\frac{\partial A}{\partial t}+\alpha U\frac{\partial U}{\partial z}+\frac{1}{\rho}\frac{\partial p}{\partial z}=\frac{2}{\rho R}\mu\left[\frac{\partial v_z}{\partial r}\right]_R \quad (1)$$

$$\frac{\partial A}{\partial t}+\frac{\partial (UA)}{\partial z}=0 \quad (2)$$

where $A(z,t)$ is the cross-sectional area of the artery, $R(z,t)$ the arterial radius, $U(z,t)$ a mean velocity in the z direction, $p(z,t)$ the pressure, ρ the blood density, μ the blood viscosity, and α a parameter that accounts for the fact that averaged quantities are conserved. The value of α is a constant for a given velocity profile [6][7]. It should be noted that in the right side of (1), $\mu\left[\frac{\partial v_z}{\partial r}\right]_R$ corresponds to the force exerted by the wall on the blood, that is, *WSS* with the opposite sign.

In the case that one is provided with the data of A and $\frac{\partial p}{\partial z}$ for all values of z of the tube and for every instant t, and a boundary condition for U (*i.e.* U in one of the extremes of the tube for every instant), the system (1)–(2) can be numerically solved to obtain U and *WSS* for all values of z and t.

B. Surgical instrumentation

The experiment was done in an adult Corrediale-Romey Marsh sheep of approximately 62 kg and 3 years of age, in total agree with the established norms in the Institutional Animal Care and Use Committee (Universidad Favaloro, NIH-PHS Nro. A5556-1) and the Guide for the Care and Use of Laboratory Animals published by U.S. National Research Council (National Academy Press, Washington, D.C. 1996).

Under pre–medication with acepromazine maleate (0.2 mg/kg IM) general anaesthesia was induced with sodium thiopental (20 mg/kg IV), and maintained with halothane (1.5–2% in pure oxygen at 2.5 L/min) under assisted mechanic ventilation (Neumovent 910, TECME SA, Crdoba, Argentina). The ventilation was controlled during all the experiment using positive pressure at a frequency of 12 cycles per minute and a tidal volume of 15 mL/kg, adjusting for maintaining a CO_2 of 25–30 mmHg (Siemens–Elema capnograph E336E, Sweden). The heart rate and the blood oxygen saturation were continually monitored with a pulse oxymeter (Novametrix, model 5154, Medical System Inc, Wallingford, Connecticut).

After a thoracotomy was done in the forth left intercostal space, two pairs of ultrasonic transducers (2 mm, 5 MHz) were implanted for measuring the external aortic diameter, one in the middle third of the descendent thoracic aorta and the other eight centimetres distal form this. In this way, the tapering of the aorta is taken into account. Through canalization of the femoral artery, a 6 French pressure microtransducer (Gaeltec Ltd, UK) was introduced, which after verifying by palpation that its endovascular position corresponded with the first diameter transducers, was fixed in the exterior. The instrumentation also included an electromagnetic flow transducer (probe 20 A) implanted a few millimetres proximal to the first pair of diameter transducers, connected to a flow–meter (model T206, Transonic Systems Inc, Ithaka, New York, USA).

C. Data acquisition and preparation

The aortic pressure, diameters and flow signals were sampled at 200 Hz in a computer (PC Pentium II) equipped with a multichannel analogical–digital converter of 12–bits (LabPC 1200, National Instruments, Austin, Texas, USA) using a specific software developed in the Department of Electronics of the Universidad Favaloro. From all the signals, the data of a stable period was selected.

Assuming that the aorta tapering is linear, and since we are provided with $A(t)$ at the inlet and the outlet of the tube, the data of A in the selected period and for all values of z was obtained. Then, assuming the pressure gradient as linear, that mean pressure in the segment length drops 0.2 mmHg approximately [8][9], and that elasticity obtained form the p–A relationship in the proximal extreme of the artery is the same for all the modelled segment, the pressure gradient for all values of z in the period was obtained.

Mean velocity U in the inlet of the tube ($z = 0$) was obtained by dividing the flow signal in the selected period by the probe cross-sectional area.

D. Numerical resolution

The system of equations was solved numerically with the Runge–Kutta method and was programmed in MATLAB. The discretization consisted in 148 points for z axis and 148 points for t ($\Delta t = 5 \times 10^{-3}$ s and $\Delta z = 5.4 \times 10^{-4}$ m). The length of the tube was $L = 8$ cm (the real distance between diameter transducers), and elasticity value was $E = 2.65 \times 10^6$ Pa/m, obtained from the p–D relationships (consistent with previous validated values [10]).

As a final result, $U(z,t)$ and $WSS(z,t)$ were obtained.

III. Results

First, the model was tested with well known situations, comparing its results with those of their analytical solution. For the case of a tube with no tapering, steady flow and lineal pressure gradient (Poiseuille's flow) the results where the same in both analytical and numerical solutions. Then, we allowed the tube to be slightly tapered, and obtained the analytical and numerical solutions with steady flow (all input quantities were the average values for the selected period from experimental data. In Fig. 1 we show this comparison. It

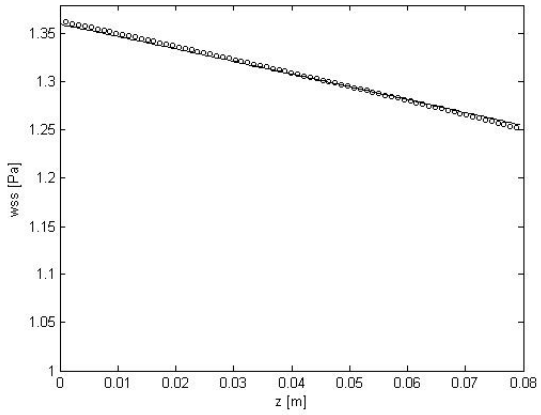

Fig. 1. *WSS* as a function of z for the case of steady flow and tapered tube. Dots correspond to numerical solution and solid line to the analytical one.

can be seen that the numerical model estimates considerably the analytical solution, with a maximum error of 0.17%.

In Fig. 2 the signals of pressure (grey line) and mean velocity at the inlet of the segment (black line) for the selected period obtained experimentally are shown.

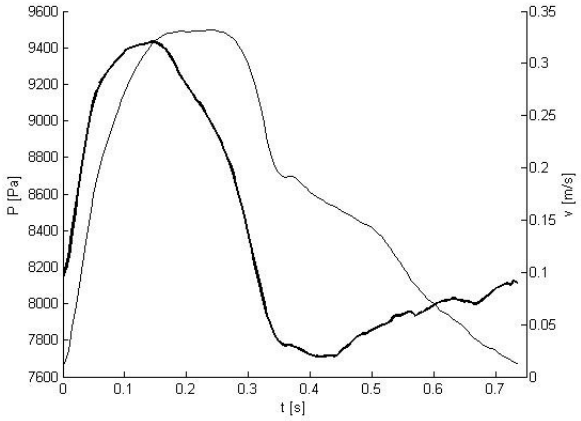

Fig. 2. Pressure (grey line) and mean velocity (black line) at the inlet of the segment.

In Fig. 3, *WSS* as a function of time and axial position with $\alpha = 4/3$ (parabolic profile) is shown.

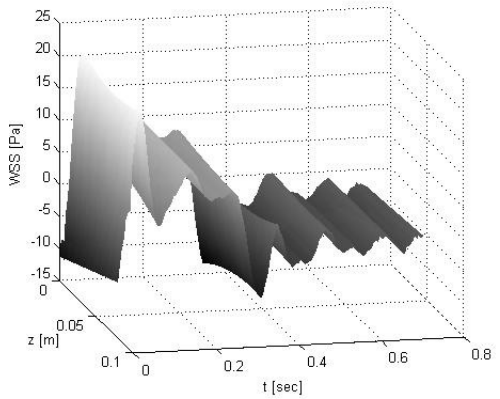

Fig. 3. *WSS* at the inlet of the tube.

Mean values of *WSS* are similar to those found in bibliography [5]. However, it is remarkable that peak values of *WSS*, which are ignored in steady flow models, are at least one order higher that the *WSS* mean values.

We compared the distribution of mean *WSS* with that obtained for the steady flow and rigid wall case (inputs were the mean values of the signals) for the same tapering condition. Differences are considerable Fig. 4. This suggests that, using steady flow and rigid walls, mean *WSS* is overestimated.

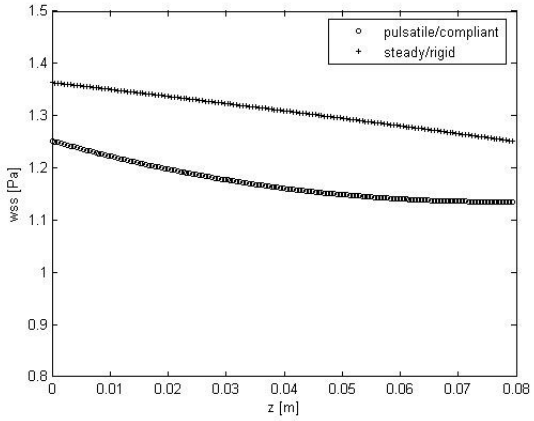

Fig. 4. Comparison of the distribution of mean *WSS* with that obtained for the steady flow and rigid wall case.

Another measure of *WSS* that represents the wave form and, in particular, the proportion of positive and negative shear is the oscillatory shear index (*OSI*) [11] [12] defined as:

$$OSI = \frac{\int_0^T |\tau^-| \, dt}{\int_0^T |\tau| \, dt} \tag{3}$$

where T is the cycle period, τ is the instantaneous shear stress and τ^- is the portion of the shear stress acting in the direction opposite the mean shear stress. As an example, *OSI* value for *WSS* at the inlet of the tube (Fig. 3) was 0.3920, which indicates that oscillations in shear stress are considerable and should be taken into account as an important feature.

Finally, since the calculations depend on the parameter α, which is a constant for a given velocity profile, we proposed to compare results for a certain range of α. In Fig. 5, mean *WSS* and peak *WSS* at the inlet of the tube as a function of α are shown. It is important to note that for two of the most commonly used profiles, such as the parabolic profile ($\alpha = 4/3$) [6][13] and the constant one ($\alpha = 1$) [6], differences are negligible. More generally, in a bigger range of α, mean *WSS* appears not to be affected, whereas for large values of α, peak *WSS* is modified considerably.

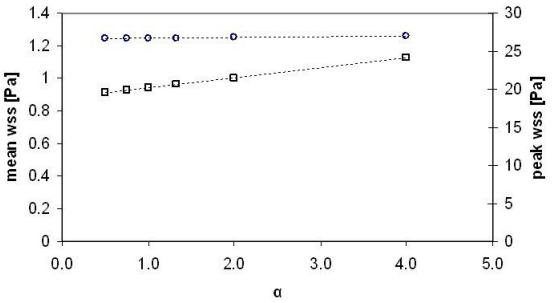

Fig. 5. Mean *WSS* (circles) and peak *WSS* (squares) as a function of the parameter α.

IV. DISCUSSIONS

It is accepted nowadays that the vessels segments that are more probable to develop a vascular disease are those with low or oscillatory values of *WSS* [2][3]. Actual studies consider stationary flow, rigid walls or very trivial geometries. It is then necessary to achieve a realistic model for the blood flow in arteries that may lead to the assessment of these important characteristics of *WSS*.

The proposed model resulted suitable for estimating *WSS* in simple cases such as Poiseulle's flow and stationary flow in a tapered vessel. In the case of pulsatile flow and compliant walls, time dependent *WSS* distribution was obtained in a sheep thoracic aorta with experimental data. Mean values were congruent with those found in bibliography; although it was shown that the steady solution with rigid walls for the same tapering overestimates mean *WSS*. An important characteristic to remark is that pulsatility and compliant walls introduce features such as peak values and oscillations that are not negligible and should be taken into account when evaluating *WSS* in a given artery. Peak values of *WSS* were in all cases at least one order higher than mean values. *OSI* was approximately 0.4 in all cases, which means that about 40% of the *WSS* in a period is negative. These two findings confirm that peak *WSS* and oscillations are considerable and suggest the need of using this kind of models to calculate realistic *WSS* in a vessel segment.

Since the physiological measurements needed for this model are the same that are used when calculating *WSS* classically (assuming stationary flow and rigid walls), no additional instrumentations in experimental investigations are required.

This model has the requirement that one should know a priori the velocity profile developed in the vessel for each particular situation. However, for the case of large arteries, the most common profiles assumed are the parabolic and the constant ones. For these, differences in *WSS* obtained with the model are negligible. More over, in a bigger spectrum of situations, peak *WSS* is affected considerably by the velocity profile.

As an important limitation, this model is only suitable for straight vessels with axial symmetry such as the aorta. More complicated geometries can not be studied, and another kind of focus such as finite element analysis or fluid–structure interaction must be performed.

V. CONCLUSION

We proposed a 1D model for blood flow in arteries that takes into account realistic features such as the flow pulsatility and the arterial wall compliance in order to obtain wall shear stress in the artery. The model was solved numerically and was validated with stationary cases. We obtained the time-dependent *WSS* distribution in a sheep thoracic aorta segment with experimental data. Results showed that peak values of wall shear stress and oscillations are considerable and should be studied with this kind of models when trying to evaluate shear stress in a vessel segment and trying to correlate it with normal and abnormal behavior of the vessel, such as a dysfunction or a disease.

The importance of this model is that it is suitable for practice since it is simple, it complains realistic features of blood flow, and can be used with common clinical measurements.

ACKNOWLEDGMENTS

Authors acknowledge grants PICTO 31355 and PICTO 21360 from Agencia Nacional de Promocin Cientfica y Tecnolgica in cooperation agreement with Favaloro University.

REFERENCES

[1] P. F. Davies, "Hemodynamic shear stress and the endothelium in cardiovascular pathophysiology," *Nat Clin Pract Cardiovasc Med*, vol. 6, pp. 16–26, 2009.

[2] C. G. Caro, "Discovery of the Role of Wall Shear in Atherosclerosis," *Arterioscler Thromb Vasc Biol*, vol. 29, no. 2, pp. 158–161, 2009.

[3] D. Katritsis, L. Kaiktsis, A. Chaniotis, J. Pantos, E. Efstathopoulos, and V. Marmarelis, "Wall shear stress: theoretical considerations and methods of measurement," *Prog Cardiovasc Dis*, vol. 49, no. 5, pp. 307–329, 2007.

[4] D. P. Giddens, C. K. Zarins, and S. Glagov, "Flow and atherogenesis in the human carotid bifurcation," in *Fluid Dynamics as a Localizing Factor for Atherosclerosis*, G. Schettler, Ed. Springer–Verlag, 1983.

[5] J. Humphrey, "Mechanisms of Arterial Remodeling in Hypertension: Coupled Roles of Wall Shear and Intramural Stress," *Hypertension*, vol. 52, no. 2, p. 195, 2008.

[6] A. Barnard, W. Hunt, W. Timlake, and E. Varley, "A theory of fluid flow in compliant tubes," *Biophysical Journal*, vol. 6, no. 6, pp. 717–724, 1966.

[7] S. Čanić, "Blood flow through compliant vessels after endovascular repair: wall deformations induced by the discontinuous wall properties," *Comp and Visual in Science*, vol. 4, no. 3, pp. 147–155, 2002.

[8] M. Olufsen, C. Peskin, W. Kim, E. Pedersen, A. Nadim, and J. Larsen, "Numerical simulation and experimental validation of blood flow in arteries with structured-tree outflow conditions," *Annals of Biomed Eng*, vol. 28, no. 11, pp. 1281–1299, 2000.

[9] W. W. Nichols and M. F. O'Rourke, *McDonald's blood flow in arteries*. London: Edward Arnold, 1995.

[10] D. Bia, I. Aguirre, Y. Zócalo, L. Devera, E. Cabrera Fischer, and R. Armentano, "Regional differences in viscosity, elasticity and wall buffering function in systemic arteries: pulse wave analysis of the arterial pressure-diameter relationship," *Rev Esp Cardiol*, vol. 58, pp. 167–174, 2005.

[11] M. Sharp, G. Thurston, and J. Moore, "The effect of blood viscoelasticity on pulsatile flow in stationary and axially moving tubes," *Biorheology*, vol. 33, no. 3, pp. 185–208, 1996.

[12] D. Ku, D. Giddens, C. Zarins, and S. Glagov, "Pulsatile Flow and Atherosclerosis in the Human Carotid Bifurcation, Positive Correlation between Plaque Location and Low and Oscillating Shear Stress," *Arterioscler Thromb Vasc Biol*, vol. 5, pp. 293–302, 1985.

[13] W. Akers, A. Barnard, H. Bourland, W. Hunt, W. Timlake, and E. Varley, "Numerical hydrodynamic calculations of catheter characteristics," *Biophysical Journal*, vol. 6, no. 6, pp. 725–733, 1966.